Asian Journal of Applied Sciences (ISSN: 2321 – 0893)
Volume 04 – Issue 06, December 2016

Unsteady Three-Dimensional Dusty Couette Flow Through Porous Plates with Heat Transfer and Periodic Suction

C. Loganathan, S. Gomathi*

Department of Mathematics, Maharaja Arts and Science College,
Coimbatore 641014, Tamilnadu, India

Corresponding author's email : gomathi_math [AT] yahoo.com

ABSTRACT : ***The unsteady three-dimensional Couette flow of a viscous incompressible fluid between two porous flat plates with uniform injection and periodic suction has been investigated. Perturbation technique has been used to obtain approximate solutions for the velocity and temperature fields, skin friction and Nusselt number. The velocity and temperature profiles have been plotted to study the effects of different non-dimensional parameters on them. Increasing mass concentration parameter results in an increase in the main velocity. Increase in the frequency parameter results in flattening of the main velocity profiles. The effects of other non-dimensional parameters have also been studied. Furthermore, skin friction and Nusselt number have been tabulated for different values of the non-dimensional parameters.***

Keywords: Slip flow regime, unsteady, porous medium,Couette flow, dusty fluid

1. INTRODUCTION

Dusty Couette flows are a part of many industrial processes including transpiration cooling, filtration and drying. Some of the areas of application of these flows are in oil recovery, aerodynamics, inverted pendulum and geothermal springs [9]. The steady two-dimensional plane Couette flow with transpiration cooling for uniform injection and suction at the porous plates for a clear fluid has been discussed in Eckert [4].

The steady Couette flow plates with transverse sinusoidal injection of the fluid at the stationary plate and the constant suction at the plate in motion have been studied by Singh [10] and have further extended for dusty fluid by Govindarajan et al. [6] and with chemical reaction by Ahmed et al. [1]. The study Couette flow for dusty fluid with heat transfer with an exponential injection at the uniform plate and a constant suction at the stationary plate has been studied by Gireesha et al. [5].

The flow and heat transfer in Couette flow for micro and nano channels have been studied by Jiji and Yazdi [8] and Zhang [11] respectively. Heat transfer in unsteady Couette flow for a dusty gas was first studied by Datta and Mishra [3]. The buoyancy effects in Couette flow were studied by Choi et al. [2].

The application of the transverse sinusoidal injection or suction velocity in the unsteady problem of transpiration cooling for a clear fluid was studied by Guria and Jana [7]. The present work aims to extend this work for dusty fluid with slip boundary condition at the suction plate and natural convection.

2. FLOW DESCRIPTION AND GOVERNING EQUATIONS

The flow under investigation has been modelled as an unsteady three-dimensional flow of a viscous, incompressible, dusty fluid between two horizontal porous flat plates separated by a distance 'd' in a slip flow regime with uniform suction at the stationary plate and periodic suction at the plate in motion. The upper plate is assumed to be the one in motion with uniform velocity U in the direction of the flow. The Cartesian coordinate system is chosen with its origin on the lower stationary plate, x^*- axis in the direction of the flow, y^*- axis taken perpendicular to the plate and directed into fluid flowing in laminar regime with a uniform free stream velocity U and z^*- axis is taken normal to the x^*y^*- plane.

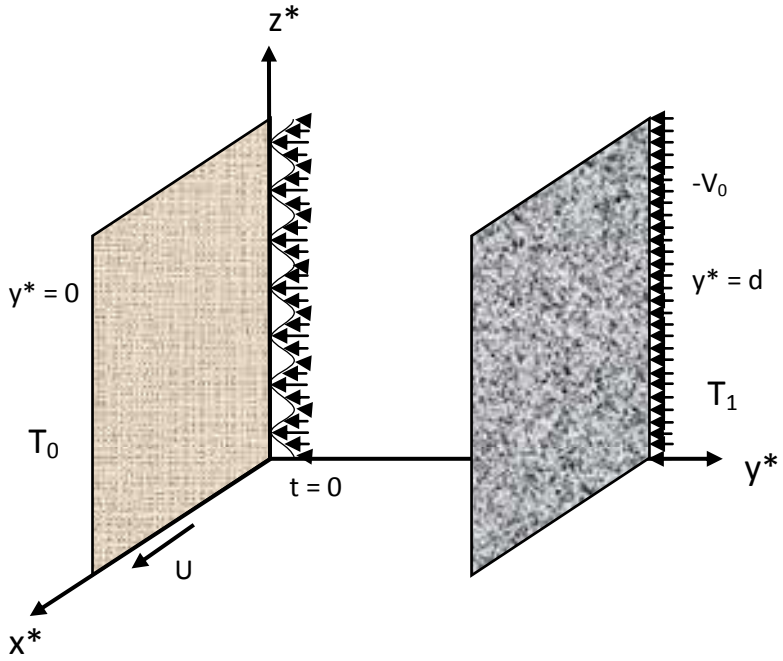

Figure 1: *Couette dusty flow with constant injection and periodic suction at the porous plates*

The upper plate is subjected to a constant injection $-V_0$ and the lower plate to a transverse sinusoidal time dependent suction velocity distribution of the form

$$v^* = -V_0\left[1+\varepsilon\cos\left(\frac{\pi z^*}{d^*}-ct^*\right)\right] \quad (1)$$

where $\varepsilon(\ll 1)$ is the amplitude of the suction velocity as shown in Fig 1. The distance between the plates is taken equal to the suction velocity. The slip condition is assumed for the fluid phase and similar slip condition is also assumed for the particle phase.

Denoting dimensional velocity components as u^*, v^* and w^*in the directions x^*, y^* and z^*axes respectively for the fluid phase, u_p^*, v_p^* and w_p^* in the directions x^*, y^* and z^*axes respectively for the particle phase and T^* and T_p^* for the temperature of the fluid and particle phase respectively, the governing equations are given as:

For fluid phase:

$$\frac{\partial v^*}{\partial y^*}+\frac{\partial w^*}{\partial z^*} = 0 \quad (2)$$

$$\frac{\partial u^*}{\partial t^*}+v^*\frac{\partial u^*}{\partial y^*}+w^*\frac{\partial u^*}{\partial z^*} = \upsilon\left(\frac{\partial^2 u}{\partial y^{*2}}+\frac{\partial^2 u}{\partial z^{*2}}\right)+g\beta_T(T^*-T_d^*)+\frac{KN_0}{\rho}\left(u_p^*-u^*\right) \quad (3)$$

$$\frac{\partial v^*}{\partial t^*}+v^*\frac{\partial v^*}{\partial y^*}+w^*\frac{\partial v^*}{\partial z^*} = \upsilon\left(\frac{\partial^2 v}{\partial y^{*2}}+\frac{\partial^2 v}{\partial z^{*2}}\right)+\frac{\partial p^*}{\partial y^*}+\frac{KN_0}{\rho}\left(v_p^*-v^*\right) \quad (4)$$

$$\frac{\partial w^*}{\partial t^*}+v^*\frac{\partial w^*}{\partial y^*}+w^*\frac{\partial w^*}{\partial z^*} = \upsilon\left(\frac{\partial^2 w}{\partial y^{*2}}+\frac{\partial^2 w}{\partial z^{*2}}\right)+\frac{\partial p^*}{\partial z^*}+\frac{KN_0}{\rho}\left(w_p^*-w^*\right) \quad (5)$$

$$\rho C_p\left(\frac{\partial T^*}{\partial t^*}+v^*\frac{\partial T^*}{\partial y^*}+w^*\frac{\partial T^*}{\partial z^*}\right) = \kappa\left(\frac{\partial^2 T}{\partial y^{*2}}+\frac{\partial^2 T}{\partial z^{*2}}\right)+\frac{\rho_p C_s}{\Gamma_T}\left(v_p^*-v^*\right) \quad (6)$$

For particle phase:

$$\frac{\partial v_p^*}{\partial y^*}+\frac{\partial w_p^*}{\partial z^*} = 0 \quad (7)$$

$$\frac{\partial u_p^*}{\partial t^*}+v_p^*\frac{\partial u_p^*}{\partial y^*}+w_p^*\frac{\partial u_p^*}{\partial z^*} = \frac{K}{m_p}\left(u^*-u_p^*\right) \quad (8)$$

$$\frac{\partial v_p^*}{\partial t^*}+v_p^*\frac{\partial v_p^*}{\partial y^*}+w_p^*\frac{\partial v_p^*}{\partial z^*} = \frac{K}{m_p}\left(v^*-v_p^*\right) \quad (9)$$

$$\frac{\partial w_p^*}{\partial t^*} + v_p^* \frac{\partial w_p^*}{\partial y^*} + w_p^* \frac{\partial w_p^*}{\partial z^*} = \frac{K}{m_p}\left(w^* - w_p^*\right) \quad (10)$$

$$\frac{\partial T_p^*}{\partial t^*} + v_p^* \frac{\partial T_p^*}{\partial y^*} + w_p^* \frac{\partial T_p^*}{\partial z^*} = \frac{1}{\Gamma_p}\left(T^* - T_p^*\right) \quad (11)$$

where all the symbols have their usual meanings and are given in the Appendix.

The corresponding boundary conditions are:

$$u^* = L_1^* \frac{\partial u^*}{\partial y^*};\quad v^* = -\mathrm{V}_0\left[1 + \varepsilon \cos\left(\frac{\pi z^*}{\mathrm{d}^*} - \mathrm{ct}^*\right)\right];\quad w^* = L_2^* \frac{\partial w^*}{\partial y^*};\quad T^* = T_0$$
$$u_p^* = L_1^* \frac{\partial u_p^*}{\partial y^*};\quad v_p^* = -\mathrm{V}_0\left[1 + \varepsilon \cos\left(\frac{\pi z^*}{\mathrm{d}^*} - \mathrm{ct}^*\right)\right];\quad w_p^* = L_2^* \frac{\partial w_p^*}{\partial y^*};\quad T_p^* = T_0 \quad \text{at} \quad y = 0 \quad (12)$$

$$u^* = U; v_p^* = -\mathrm{V}_0;\quad w^* = 0;\ T^* = T_1$$
$$u_p^* = U;\quad v_p^* = -\mathrm{V}_0;\quad w_p^* = 0;\ T_p^* = T_1 \quad \text{at} \quad y = d \quad (13)$$

where $L_1^*, L_2^* = \left(\frac{2-r}{r}\right)L$ and $L = \mu\left(\frac{\pi}{2P\rho}\right)^{1/2}$ is the mean free path and r is the Maxwell's reflection coefficient.

By introducing the following non-dimensional parameters:

$y = \frac{y^*}{d}$; $z = \frac{z^*}{d}$; $t = ct^*$; $p = \frac{p^*}{\rho V_0^2}$; $u = \frac{u^*}{U}$; $v = \frac{v^*}{V_0}$; $w = \frac{w^*}{V_0}$; $\theta = \frac{T^* - T_d^*}{T_0^* - T_d^*}$; $\Gamma_p = \frac{\Lambda d}{V_0}$; $u_p = \frac{u_p^*}{U}$; $v_p = \frac{v_p^*}{V_0}$; $w_p = \frac{w_p^*}{V_0}$;

$\theta_p = \frac{T_p^* - T_d^*}{T_0^* - T_d^*}$; $Re = \frac{V_0 d}{\upsilon}$, Reynolds number; $Pr = \frac{\mu C_p}{\kappa}$, Prandtl number; $f = \frac{N_0 m}{\rho}$, Mass concentration parameter;

$h = \frac{L}{d}$, Slip parameter, $m = \frac{T_1^* - T_d^*}{T_0^* - T_d^*}$, Temperature parameter; $Gr = \frac{g\beta_T d(T_0^* - T_d^*)}{UV_0}$, Grashof number; $\lambda = \frac{cd^2}{\upsilon}$,

Frequency parameter ; $\Lambda = \frac{m_p V_0}{dK}$, Relaxation time parameter. (14)

The governing equations (2) - (11) can be rewritten in non-dimensional form as follows:

$$\frac{\partial v}{\partial y} + \frac{\partial w}{\partial z} = 0 \quad (15)$$

$$\lambda\frac{\partial u}{\partial t} + Re\left(v\frac{\partial u}{\partial y} + w\frac{\partial u}{\partial z}\right) = \left(\frac{\partial^2 u}{\partial y^2} + \frac{\partial^2 u}{\partial z^2}\right) + ReGr\theta + \frac{fRe}{\Lambda}\left(u_p - u\right) \quad (16)$$

$$\lambda\frac{\partial v}{\partial t} + Re\left(v\frac{\partial v}{\partial y} + w\frac{\partial v}{\partial z}\right) = \left(\frac{\partial^2 v}{\partial y^2} + \frac{\partial^2 v}{\partial z^2}\right) - Re\frac{\partial p}{\partial y} + \frac{fRe}{\Lambda}\left(v_p - v\right) \quad (17)$$

$$\lambda\frac{\partial w}{\partial t} + Re\left(v\frac{\partial w}{\partial y} + w\frac{\partial w}{\partial z}\right) = \left(\frac{\partial^2 w}{\partial y^2} + \frac{\partial^2 w}{\partial z^2}\right) - Re\frac{\partial p}{\partial z} + \frac{fRe}{\Lambda}\left(w_p - w\right) \quad (18)$$

$$\lambda Pr\frac{\partial \theta}{\partial t} + RePr\left(v\frac{\partial \theta}{\partial y} + w\frac{\partial \theta}{\partial z}\right) = \left(\frac{\partial^2 \theta}{\partial y^2} + \frac{\partial^2 \theta}{\partial z^2}\right) + ReGr\theta + \frac{2}{3}\frac{fRe}{\Lambda}\left(\theta_p - \theta\right) \quad (19)$$

$$\frac{\partial v_p}{\partial y} + \frac{\partial w_p}{\partial z} = 0 \quad (20)$$

$$\lambda\frac{\partial u_p}{\partial t} + Re\left(v_p\frac{\partial u_p}{\partial y} + w_p\frac{\partial u_p}{\partial z}\right) = \frac{Re}{\Lambda}\left(u - u_p\right) \quad (21)$$

$$\lambda\frac{\partial v_p}{\partial t} + Re\left(v_p\frac{\partial v_p}{\partial y} + w_p\frac{\partial v_p}{\partial z}\right) = \frac{Re}{\Lambda}\left(v - v_p\right) \quad (22)$$

$$\lambda\frac{\partial w_p}{\partial t} + Re\left(v_p\frac{\partial w_p}{\partial y} + w_p\frac{\partial w_p}{\partial z}\right) = \frac{Re}{\Lambda}\left(w - w_p\right) \quad (23)$$

$$\lambda\frac{\partial \theta_p}{\partial t} + Re\left(v_p\frac{\partial \theta_p}{\partial y} + w_p\frac{\partial \theta_p}{\partial z}\right) = \frac{Re}{\Lambda}\left(\theta - \theta_p\right) \quad (24)$$

The corresponding boundary conditions are

$$u = h\frac{\partial u}{\partial y};\quad v = -\mathrm{S}[1 + \varepsilon\ \cos(\pi z - t)];\quad w = h\frac{\partial w}{\partial y};\quad \theta = 1$$
$$u_p = h\frac{\partial u_p}{\partial y};\quad v_p = -\mathrm{S}[1 + \varepsilon\ \cos(\pi z - t)];\quad w_p = h\frac{\partial w_p}{\partial y};\quad \theta_p = 1 \quad \text{at} \quad y = 0 \quad (25)$$

$$u = 1;\ v = -1;\quad w = 0\ ;\ \theta = m$$
$$u_p = 1; v_p = -1;\quad w_p = 0;\ \theta_p = m \quad \text{at} \quad y = 1 \quad (26)$$

where $S = 1$.

3. SOLUTION OF THE PROBLEM

When the amplitude of oscillation in the suction velocity is small ($\varepsilon \ll 1$), we can assume u, v, w, θ, u_p, v_p, w_p, θ_p and p in the following form to solve the differential equations (15) - (24).

$$\begin{aligned}
u(y,z,t) &= u_0(y) + \varepsilon u_1(y,z,t) + \varepsilon^2 u_2(y,z,t) + \cdots \\
v(y,z,t) &= v_0(y) + \varepsilon v_1(y,z,t) + \varepsilon^2 v_2(y,z,t) + \cdots \\
w(y,z,t) &= w_0(y) + \varepsilon w_1(y,z,t) + \varepsilon^2 w_2(y,z,t) + \cdots \\
\theta(y,z,t) &= \theta_0(y) + \varepsilon \theta_1(y,z,t) + \varepsilon^2 \theta_2(y,z,t) + \cdots \\
u_p(y,z,t) &= u_{p_0}(y) + \varepsilon u_{p_1}(y,z,t) + \epsilon^2 u_{p_2}(y,z,t) + \cdots \\
v_p(y,z,t) &= v_{p_0}(y) + \varepsilon v_{p_1}(y,z,t) + \varepsilon^2 v_{p_2}(y,z,t) + \cdots \\
w_p(y,z,t) &= w_{p_0}(y) + \varepsilon w_{p_1}(y,z,t) + \varepsilon^2 w_{p_2}(y,z,t) + \cdots \\
\theta_p(y,z,t) &= \theta_{p_0}(y) + \varepsilon \theta_{p_1}(y,z,t) + \varepsilon^2 \theta_{p_2}(y,z,t) + \cdots \\
p(y,z,t) &= p_0(y) + \varepsilon p_1(y,z,t) + \varepsilon^2 p_2(y,z,t) + \cdots
\end{aligned} \tag{27}$$

When $\varepsilon = 0$, the differential equations (15) - (24) pertaining to two dimensional flow are obtained as:

$$v_0' = 0 \tag{28}$$

$$u_0'' - Rev_0u_0' + ReGr\theta_0 + \frac{fRe}{\Lambda}\left(u_{p_0} - u_0\right) = 0 \tag{29}$$

$$p_0' = \frac{f}{\Lambda}\left(v_{p_0} - v_0\right) \tag{30}$$

$$w_0'' - Rev_0w_0' + \frac{fRe}{\Lambda}\left(w_{p_0} - w_0\right) = 0 \tag{31}$$

$$\theta_0'' - RePrv_0\theta_0' + \frac{2}{3}\frac{fRe}{\Lambda}\left(\theta_{p_0} - \theta_0\right) = 0 \tag{32}$$

$$v_{p_0}' = 0 \tag{33}$$

$$v_0u_{p_0}' + \frac{1}{\Lambda}\left(u_{p_0} - u_0\right) = 0 \tag{34}$$

$$v_{p_0} = v_0 \tag{35}$$

$$v_0w_{p_0}' + \frac{1}{\Lambda}\left(w_{p_0} - w_0\right) = 0 \tag{36}$$

$$v_0\theta_{p_0}' + \frac{1}{\Lambda}\left(\theta_{p_0} - \theta_0\right) = 0 \tag{37}$$

subject to the boundary conditions

$$u_0 = h\frac{\partial u_0}{\partial y};\quad v_0 = -S;\quad w_0 = h\frac{\partial w_0}{\partial y};\quad \theta_0 = 1$$
$$u_{p_0} = h\frac{\partial u_{p_0}}{\partial y};\quad v_{p_0} = -\mathrm{S};\quad w_{p_0} = h\frac{\partial w_{p_0}}{\partial y};\quad \theta_{p_0} = 1 \quad \text{at} \quad y = 0 \tag{38}$$

$$u_0 = 1;\quad v_0 = -1;\quad w_0 = 0;\quad \theta_0 = m$$
$$u_{p_0} = 1;\quad v_{p_0} = -1;\quad w_{p_0} = 0;\quad \theta_{p_0} = m \quad \text{at} \quad y = 1 \tag{39}$$

The solutions for the equations (28), (30), (33) and (35) are

$$v_0 = v_{p_0} = -1 \tag{40}$$

$$p_0' = 0 \tag{41}$$

Substituting $S = 1$ and equations (40) - (41) in equations (28) - (37) and rearranging as done in Govindarajan et al. [6], we get

$$-\Lambda u_0''' + (1 - Re\Lambda)u_0'' + Re(1+f)u_0' + ReGr\theta_0 - \Lambda ReGr\theta_0' = 0 \tag{42}$$

$$-\Lambda w_0''' + (1 - Re\Lambda)w_0'' + Re(1+f)w_0' = 0 \tag{43}$$

$$-\Lambda\theta_0''' + (1 - Re\Lambda)\theta_0'' + Re\left(Pr + \frac{2}{3}f\right)\theta_0' = 0 \tag{44}$$

$$-\Lambda u_{p_0}' + u_{p_0} = u_0 \tag{45}$$

$$-\Lambda w_{p_0}' + w_{p_0} = w_0 \tag{46}$$

$$-\Lambda\theta_{p_0}' + \theta_{p_0} = \theta_0 \tag{47}$$

The solution to the remaining equations are:

$$w_0 = w_{p_0} = 0 \tag{48}$$

$$\theta_0 = C_1e^{J_1y} + C_2e^{J_2y} + C_3 \tag{49}$$

$$\theta_{p_0} = C_0 e^{\frac{y}{\Lambda}} + \frac{C_1}{(1-\Lambda J_1)} e^{J_1 y} + \frac{C_2}{(1-\Lambda J_2)} e^{J_2 y} + C_3 \quad (50)$$

$$u_0 = C_4 e^{J_3 y} + C_5 e^{J_4 y} + C_6 + C_7 e^{J_1 y} + C_8 e^{J_2 y} + C_9 y \quad (51)$$

$$u_{p_0} = C_{10} e^{\frac{y}{\Lambda}} + \frac{C_4}{(1-\Lambda J_3)} e^{J_3 y} + \frac{C_5}{(1-\Lambda J_4)} e^{J_4 y} + C_6 + \Lambda C_9 + \frac{C_7}{(1-\Lambda J_1)} e^{J_1 y} + \frac{C_8}{(1-\Lambda J_2)} e^{J_2 y} + C_9 y \quad (52)$$

The unsteady state equations are:

$$\frac{\partial v_1}{\partial y} + \frac{\partial w_1}{\partial z} = 0 \quad (53)$$

$$\lambda \frac{\partial u_1}{\partial t} + Re\left(-S\frac{\partial u_1}{\partial y} + v_1 \frac{\partial u_0}{\partial y}\right) = \left(\frac{\partial^2 u_1}{\partial y^2} + \frac{\partial^2 u_1}{\partial z^2}\right) + ReGr\theta_1 + \frac{fRe}{\Lambda}\left(u_{p_1} - u_1\right) \quad (54)$$

$$\lambda \frac{\partial v_1}{\partial t} + Re\left(-S\frac{\partial v_1}{\partial y}\right) = \left(\frac{\partial^2 v_1}{\partial y^2} + \frac{\partial^2 v_1}{\partial z^2}\right) - Re\frac{\partial p_1}{\partial y} + \frac{fRe}{\Lambda}\left(v_{p_1} - v_1\right) \quad (55)$$

$$\lambda \frac{\partial w_1}{\partial t} + Re\left(-S\frac{\partial w_1}{\partial y}\right) = \left(\frac{\partial^2 w_1}{\partial y^2} + \frac{\partial^2 w_1}{\partial z^2}\right) - Re\frac{\partial p_1}{\partial z} + \frac{fRe}{\Lambda}\left(w_{p_1} - w_1\right) \quad (56)$$

$$\lambda Pr\frac{\partial \theta_1}{\partial t} + RePr\left(-S\frac{\partial \theta_1}{\partial y} + v_1\frac{\partial \theta_0}{\partial y}\right) = \left(\frac{\partial^2 \theta_1}{\partial y^2} + \frac{\partial^2 \theta_1}{\partial z^2}\right) + \frac{2}{3}\frac{fRe}{\Lambda}\left(\theta_{p_1} - \theta_1\right) \quad (57)$$

$$\frac{\partial v_{p_1}}{\partial y} + \frac{\partial w_{p_1}}{\partial z} = 0 \quad (58)$$

$$\lambda \frac{\partial u_{p_1}}{\partial t} + Re\left(-S\frac{\partial u_{p_1}}{\partial y} + v_{p_1}\frac{\partial u_{p_0}}{\partial y}\right) = \frac{Re}{\Lambda}\left(u_1 - u_{p_1}\right) \quad (59)$$

$$\lambda \frac{\partial v_{p_1}}{\partial t} + Re\left(-S\frac{\partial v_{p_1}}{\partial y}\right) = \frac{Re}{\Lambda}\left(v_1 - v_{p_1}\right) \quad (60)$$

$$\lambda \frac{\partial w_{p_1}}{\partial t} + Re\left(-S\frac{\partial w_{p_1}}{\partial y}\right) = \frac{Re}{\Lambda}\left(w_1 - w_{p_1}\right) \quad (61)$$

$$\lambda \frac{\partial \theta_{p_1}}{\partial t} + Re\left(-S\frac{\partial \theta_{p_1}}{\partial y} + v_{p_1}\frac{\partial \theta_{p_0}}{\partial y}\right) = \frac{Re}{\Lambda}\left(\theta_1 - \theta_{p_1}\right) \quad (62)$$

The boundary conditions become

$$u_1 = h\frac{\partial u_1}{\partial y};\quad v_1 = -\mathrm{S}\big(cos(\pi z - t)\big);\quad w_1 = h\frac{\partial w_1}{\partial y};\quad \theta_1 = 0$$

$$u_{p_1} = h\frac{\partial u_{p_1}}{\partial y};\quad v_{p_1} = -\mathrm{S}\big(cos(\pi z - t)\big);\quad w_{p_1} = h\frac{\partial w_{p_1}}{\partial y};\quad \theta_{p_1} = 0 \quad \text{at} \quad y = 0 \quad (63)$$

$$u_1 = v_1 = w_1 = \theta_1 = u_{p_1} = v_{p_1} = w_{p_1} = \theta_{p_1} = 0 \quad \text{at} \quad y = 1 \quad (64)$$

In order to solve these partial differential equations u_1, v_1, w_1, θ_1, u_{p_1}, v_{p_1}, w_{p_1}, θ_{p_1} and p_1 are assumed to be of the following complex form:

$$\begin{aligned} u_1(y,z,t) &= u_{11}(y)e^{i(\pi z - t)} \\ v_1(y,z,t) &= v_{11}(y)e^{i(\pi z - t)} \\ w_1(y,z,t) &= \frac{i}{\pi}v'_{11}(y)e^{i(\pi z - t)} \\ \theta_1(y,z,t) &= \theta_{11}(y)e^{i(\pi z - t)} \\ u_{p_1}(y,z,t) &= u_{p_{11}}(y)e^{i(\pi z - t)} \\ v_{p_1}(y,z,t) &= v_{p_{11}}(y)e^{i(\pi z - t)} \\ w_{p_1}(y,z,t) &= \frac{i}{\pi}v_{p'_{11}}(y)e^{i(\pi z - t)} \\ \theta_{p_1}(y,z,t) &= \theta_{p_{11}}(y)e^{i(\pi z - t)} \\ p_1(y,z,t) &= p_{11}(y)e^{i(\pi z - t)} \end{aligned} \quad (65)$$

Now using $S = 1$ and (65) in equations (53) - (62) and rearranging as before, we get

$$u''_{11} + Reu'_{11} + (-\pi^2 + i\lambda)u_{11} + \frac{fRe}{\Lambda}\left(u_{p_{11}} - u_{11}\right) = -ReGr\theta_{11} + Rev_{11}u'_0 \quad (66)$$

$$v''_{11} + Rev'_{11} + (-\pi^2 + i\lambda)v_{11} + \frac{fRe}{\Lambda}\left(v_{p_{11}} - v_{11}\right) = Rep'_{11} \quad (67)$$

$$v'''_{11} + Rev''_{11} + (-\pi^2 + i\lambda)v'_{11} + \frac{fRe}{\Lambda}\left(v_{p'_{11}} - v'_{11}\right) = \pi^2 Rep'_{11} \quad (68)$$

$$\theta''_{11} + Re\theta'_{11} + (-\pi^2 + i\lambda Pr)\theta_{11} + \frac{2}{3}\frac{fRe}{\Lambda}\left(\theta_{p_{11}} - \theta_{11}\right) = Rev_{11}\theta'_0 \quad (69)$$

$$-\Lambda u_{p'_{11}} + \left(1 - \frac{i\lambda\Lambda}{Re}\right)u_{p_{11}} = u_{11} - \Lambda v_{p_{11}}u_{p'_0} \quad (70)$$

$$-\Lambda v_{p'_{11}} + \left(1 - \frac{i\lambda\Lambda}{Re}\right)v_{p_{11}} = v_{11} \quad (71)$$

$$-\Lambda v_{p_{11}}'' + \left(1 - \frac{i\lambda\Lambda}{Re}\right) v_{p_{11}}' = v_{11}' \quad (72)$$

$$-\Lambda \theta_{p_{11}}' + \left(1 - \frac{i\lambda\Lambda}{Re}\right) \theta_{p_{11}} = \theta_{11} - \Lambda v_{p_{11}} \theta_{p_0}' \quad (73)$$

Boundary conditions are

$$u_{11} = h\frac{\partial u_{11}}{\partial y}; \quad v_{11} = -1; \quad w_{11} = h\frac{\partial w_{11}}{\partial y}; \quad \theta_{11} = 0$$

$$u_{p_{11}} = h\frac{\partial u_{p_{11}}}{\partial y}; \; v_{p_{11}} = -1; \quad w_{p_{11}} = h\frac{\partial w_{p_{11}}}{\partial y}; \; \theta_{p_{11}} = 0 \quad \text{at} \quad y = 0 \quad (74)$$

$$u_{11} = v_{11} = w_{11} = \theta_{11} = u_{p_{11}} = v_{p_{11}} = w_{p_{11}} = \theta_{p_{11}} = 0 \quad \text{at} \quad y = 1 \quad (75)$$

The solutions of the equations (66) - (73) subject to boundary conditions (74) - (75) are

$$p_{11} = A_1 e^{\pi y} + A_2 e^{-\pi y} \quad (76)$$

$$v_{11} = C_{13}e^{J_8 y} + C_{14}e^{J_9 y} + C_{15}e^{J_{10} y} + C_{11}e^{J_6 y} + C_{12}e^{J_7 y} \quad (77)$$

$$v_{p_{11}} = C_{16}e^{J_{11} y} + C_{17}e^{J_6 y} + C_{18}e^{J_7 y} + C_{19}e^{J_8 y} + C_{20}e^{J_9 y} + C_{21}e^{J_{10} y} \quad (78)$$

$$w_{11} = \frac{i}{\pi}[C_{13}J_8 e^{J_8 y} + C_{14}J_9 e^{J_9 y} + C_{15}J_{10}e^{J_{10} y} + C_{11}J_6 e^{J_6 y} + C_{12}J_7 e^{J_7 y}] \quad (79)$$

$$w_{p_{11}} = \frac{i}{\pi}[C_{16}J_{11}e^{J_{11} y} + C_{17}J_6 e^{J_6 y} + C_{18}J_7 e^{J_7 y} + C_{19}J_8 e^{J_8 y} + C_{20}J_9 e^{J_9 y} + C_{21}J_{10}e^{J_{10} y}] \quad (80)$$

$$\theta_{11} = C_{22}e^{J_{12} y} + C_{23}e^{J_{13} y} + C_{24}e^{J_{14} y} + (C_{25}e^{J_6 y} + C_{26}e^{J_7 y} + C_{27}e^{J_8 y} + C_{28}e^{J_9 y} + C_{29}e^{J_{10} y} + C_{30}e^{J_{11} y})e^{J_1 y} + (C_{31}e^{J_6 y} + C_{32}e^{J_7 y} + C_{33}e^{J_8 y} + C_{34}e^{J_9 y} + C_{35}e^{J_{10} y} + C_{36}e^{J_{11} y})e^{J_2 y} + (C_{37}e^{J_6 y} + C_{38}e^{J_7 y} + C_{39}e^{J_8 y} + C_{40}e^{J_9 y} + C_{41}e^{J_{10} y} + C_{42}e^{J_{11} y})e^{J_5 y} \quad (81)$$

$$\theta_{p_{11}} = C_{43}e^{J_{11} y} + C_{44}e^{J_{12} y} + C_{45}e^{J_{13} y} + C_{46}e^{J_{14} y} + (C_{47}e^{J_6 y} + C_{48}e^{J_7 y} + C_{49}e^{J_8 y} + C_{50}e^{J_9 y} + C_{51}e^{J_{10} y} + C_{52}e^{J_{11} y})e^{J_1 y} + (C_{53}e^{J_6 y} + C_{54}e^{J_7 y} + C_{55}e^{J_8 y} + C_{56}e^{J_9 y} + C_{57}e^{J_{10} y} + C_{58}e^{J_{11} y})e^{J_2 y} + (C_{59}e^{J_6 y} + C_{60}e^{J_7 y} + C_{61}e^{J_8 y} + C_{62}e^{J_9 y} + C_{63}e^{J_{10} y} + C_{64}e^{J_{11} y})e^{J_5 y} \quad (82)$$

$$u_{11} = D_1 e^{J_8 y} + D_2 e^{J_9 y} + D_3 e^{J_{10} y} + D_4 e^{J_{12} y} + D_5 e^{J_{13} y} + D_6 e^{J_{14} y} + (D_7 e^{J_6 y} + D_8 e^{J_7 y} + D_9 e^{J_8 y} + D_{10}e^{J_9 y} + D_{11}e^{J_{10} y} + D_{12}e^{J_{11} y})e^{J_1 y} + (D_{13}e^{J_6 y} + D_{14}e^{J_7 y} + D_{15}e^{J_8 y} + D_{16}e^{J_9 y} + D_{17}e^{J_{10} y} + D_{18}e^{J_{11} y})e^{J_2 y} + (D_{19}e^{J_6 y} + D_{20}e^{J_7 y} + D_{21}e^{J_8 y} + D_{22}e^{J_9 y} + D_{23}e^{J_{10} y} + D_{24}e^{J_{11} y})e^{J_3 y} + (D_{25}e^{J_6 y} + D_{26}e^{J_7 y} + D_{27}e^{J_8 y} + D_{28}e^{J_9 y} + D_{29}e^{J_{10} y} + D_{30}e^{J_{11} y})e^{J_4 y} + (D_{31}e^{J_6 y} + D_{32}e^{J_7 y} + D_{33}e^{J_8 y} + D_{34}e^{J_9 y} + D_{35}e^{J_{10} y} + D_{36}e^{J_{11} y})e^{J_5 y} + D_{37}e^{J_6 y} + D_{38}e^{J_7 y} + D_{39}ye^{J_8 y} + D_{40}ye^{J_9 y} + D_{41}ye^{J_{10} y} + D_{42}e^{J_{11} y} \quad (83)$$

$$u_{p_{11}} = D_{43}e^{J_{11} y} + D_{44}e^{J_6 y} + D_{45}e^{J_7 y} + D_{46}e^{J_{12} y} + D_{47}e^{J_{13} y} + D_{48}e^{J_{14} y} + (D_{49}e^{J_6 y} + D_{50}e^{J_7 y} + D_{51}e^{J_8 y} + D_{52}e^{J_9 y} + D_{53}e^{J_{10} y} + D_{54}e^{J_{11} y})e^{J_1 y} + (D_{55}e^{J_6 y} + D_{56}e^{J_7 y} + D_{57}e^{J_8 y} + D_{58}e^{J_9 y} + D_{59}e^{J_{10} y} + D_{60}e^{J_{11} y})e^{J_2 y} + (D_{61}e^{J_6 y} + D_{62}e^{J_7 y} + D_{63}e^{J_8 y} + D_{64}e^{J_9 y} + D_{65}e^{J_{10} y} + D_{66}e^{J_{11} y})e^{J_3 y} + (D_{67}e^{J_6 y} + D_{68}e^{J_7 y} + D_{69}e^{J_8 y} + D_{70}e^{J_9 y} + D_{71}e^{J_{10} y} + D_{72}e^{J_{11} y})e^{J_4 y} + (D_{73}e^{J_6 y} + D_{74}e^{J_7 y} + D_{75}e^{J_8 y} + D_{76}e^{J_9 y} + D_{77}e^{J_{10} y} + D_{78}e^{J_{11} y})e^{J_5 y} + D_{79}e^{J_{11} y} + D_{80}ye^{J_8 y} + D_{81}ye^{J_9 y} + D_{82}ye^{J_{10} y} + D_{83}e^{J_8 y} + D_{84}e^{J_9 y} + D_{85}e^{J_{10} y} \quad (84)$$

Skin Friction

The skin friction at the wall due to main flow is given by:

$$\tau_x = \left(\frac{du}{dy}\right)_{y=0} = \left(\frac{du_0}{dy}\right)_{y=0} + \varepsilon\left(\frac{du_{11}}{dy}\right)_{y=0} e^{i(\pi z - t)} + O(\varepsilon^2)$$

$$= \tau_{u_0} + \varepsilon Re_x \cos(\pi z - t + \phi_x) \quad (85)$$

The skin friction at the wall due to cross flow is given by:

$$\tau_z = \left(\frac{dw}{dy}\right)_{y=0} = \left(\frac{dw_0}{dy}\right)_{y=0} + \varepsilon\left(\frac{dw_{11}}{dy}\right)_{y=0} e^{i(\pi z - t)} + O(\varepsilon^2)$$

$$= \varepsilon Re_z \cos(\pi z - t + \phi_z) \quad (86)$$

Nusselt Number

The rate of heat transfer from the plate can be calculated using the formula $q_w = -\left(\frac{\partial T}{\partial y}\right)_{y=0}$ and can be written in non-dimensional form as Nusselt number:

$$Nu = -\left(\frac{d\theta}{dy}\right)_{y=0} = -\left(\frac{d\theta_0}{dy}\right)_{y=0} - \varepsilon\left(\frac{d\theta_{11}}{dy}\right)_{y=0} e^{i(\pi z - t)} + O(\varepsilon^2)$$

$$= -\theta_0'(0) + \varepsilon Re_T \cos(\pi z - t + \phi_T) \quad (87)$$

4. NUMERICAL RESULTS

The velocity and temperature profiles have been plotted in (Fig.2-24) to study the effect of different non-dimensional parameters on the profiles. Furthermore, skin friction and Nusselt number have been tabulated (Table 2-11) for different values of non-dimensional parameters such as Grashof number (Gr), Reynolds number (Re), Prandtl number (Pr), mass concentration parameter (f), relaxation time parameter (Λ), frequency parameter (λ), Slip parameter (h) and temperature parameter (m). The main flow velocity profile and temperature profile for fluid with very little particle mass concentration have been tabulated in Table1. The results are found to be in agreement with that of Guria and Jana [7].

Increasing the relaxation time parameter (Λ) or decreasing the magnitude of Grashof number (Gr) results in a decrease in the main velocity magnitude for both fluid and particle phase (Fig.2-5). For Gr > 0 and higher Reynolds number (Re), the magnitude of main fluid and particle velocity increases with increasing Re as expected (Fig.6-7). The magnitude of main velocity decreases with increasing value of temperature parameter (m) and decreasing value of slip parameter (h) for both phases and Gr > 0 (Fig.8-11).

Increasing the mass concentration parameter (f) results in a small increase in the magnitude of main velocity for fluid phase and the increase in magnitude decreases with increasing f for the particle phase (Fig.12-13). The cross flow velocity profile flattens with decreasing relaxation time parameter (Λ) for both phases at higher values (Fig.14-15). Also, increase in slip parameter flattens the cross flow velocity profile (Fig.24). Variation of other parameters has little effect on the cross flow velocity profiles.

Increasing relaxation time parameter (Λ) flattens the particle temperature profile but increases oscillations in the fluid temperature profile (Fig.16-17). Decreasing Pr flattens the oscillations in the temperature profiles for both fluid and particle phase (Fig.18-19). Increasing mass concentration parameter (f) flattens the temperature profiles, but to a smaller extent with increasing values (Fig.20-21). Increasing the temperature parameter (m) increases the oscillations in the fluid temperature profile (Fig.22-23).

The amplitude of the shear stress and the magnitude of tangent of phase shift due to main flow increases with the increasing magnitude of Grashof number (Gr) and the increasing magnitude of difference between the temperature parameter (m) and the temperature at the opposite end (Table 3). The amplitude of the shear stress due to both main flow and cross flow decreases with increasing slip parameter (h). The tangent of phase shift increases with increasing slip parameter (h) for cross flow but decreases with increasing slip parameter (h) for main flow (Table 5 and Table 7).

The amplitude of the shear stress due to cross flow increases with increasing frequency parameter (λ) and relaxation time parameter (Λ) (Table 6). The tangent of phase shift due to cross flow mostly increases with increasing relaxation time parameter (Λ) but it decreases with increasing frequency parameter (λ). There is no general relation between the dependence of the shear stress due to main flow on the other parameters. The shear stress is dependent on the interplay between these parameters and a general trend can only be obtained for a much localized domain (Table 2-4).

The amplitude of Nusselt number decreases with increasing mass concentration parameter (f) while it increases with increasing relaxation time parameter (Λ). The tangent of the phase shift of Nusselt number follows the opposite trend with increasing f and Λ (Table10). Both the amplitude and tangent of phase shift of Nusselt number increase with increasing Prandtl number (Pr) but decrease with increasing slip parameter (h) (Table 9 and Table 11).

The amplitude of Nusselt number increases with the increasing magnitude of difference between the temperature parameter (m) and the temperature at the opposite end but it does not affect its tangent of phase shift (Table 9). Similar to the shear stress, there is no clear trend of Nusselt number with respect to Reynolds number (Re) and frequency parameter (λ). For small values of frequency parameter (λ) and Reynolds number (Re), there is a phase lag (Table 8). For other cases, there is mostly a phase lead.

5. CONCLUSION

We have extended the work of Guria and Jana [7] to study the effect of dust particles in the fluid and slip parameter on the three-dimensional unsteady couette flow of viscous incompressible fluid between two horizontal porous flat plates. A periodic suction is applied to the stationary plate and a constant injection is applied to the uniformly moving plate. The conclusions of the study are:

- Increasing the relaxation time parameter (Λ) or decreasing the magnitude of Grashof number (Gr) results in a decrease in the main velocity magnitude for both fluid and particle phase.
- The magnitude of main velocity decreases with increasing value of temperature parameter (m) and decreasing value of slip parameter (h) for both phases.
- The amplitude of the shear stress and the magnitude of tangent of phase shift due to main flow increases with increasing magnitude of Grashof number (Gr) and increasing temperature difference between the two plates.
- The cross flow velocity profile flattens with decreasing relaxation time parameter (Λ) for both phases at higher values.

- The amplitude of the shear stress due to cross flow increases with increasing frequency parameter (λ) and relaxation time parameter (Λ).
- Decreasing Pr or increasing Re flattens the oscillations in the temperature profiles for both fluid and particle phase.
- The amplitude of Nusselt number decreases with increasing mass concentration parameter (f) while it increases with increasing relaxation time parameter (Λ).

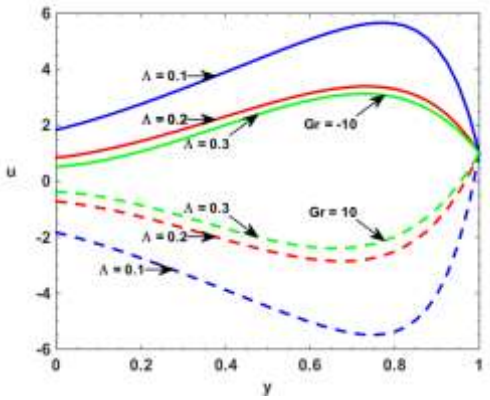

Figure 2: *Main particle velocity u vs y for λ = 5, Re = 2.5, Pr = 2, m = 1.5, h = 0.5, f = 0.2, z = 0.0, t = 0.0, ε = 0.05*

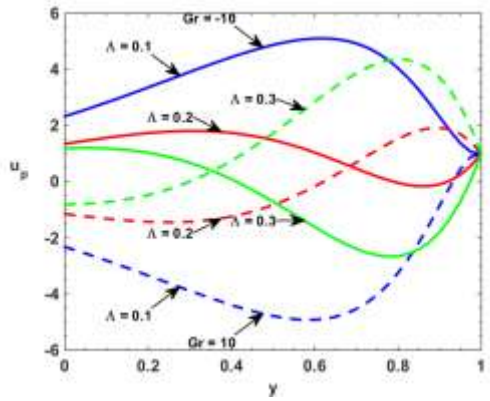

Figure 3: *Main particle velocity u_p vs y for λ = 5, Re = 2.5,Pr = 2, m = 1.5, h = 0.5, f = 0.2, z = 0.0, t = 0.0, ε = 0.05*

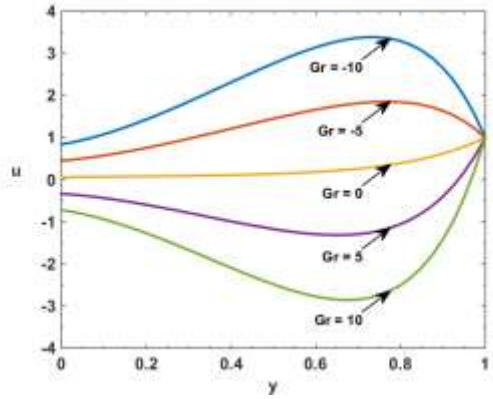

Figure 4: *Main velocity u vs y for λ = 5, Re = 2.5, Pr = 2, m = 1.5, h = 0.5, Λ = 0.2, f = 0.2, z = 0.0, t = 0.0, ε = 0.05*

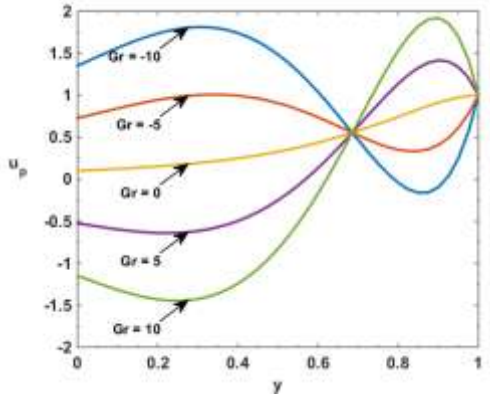

Figure 5: *Main particle velocity u_p vs y for λ = 5, Re = 2.5, Pr = 2, m = 1.5, h = 0.5, Λ = 0.2, f = 0.2, z = 0, t = 0.0, ε = 0.05*

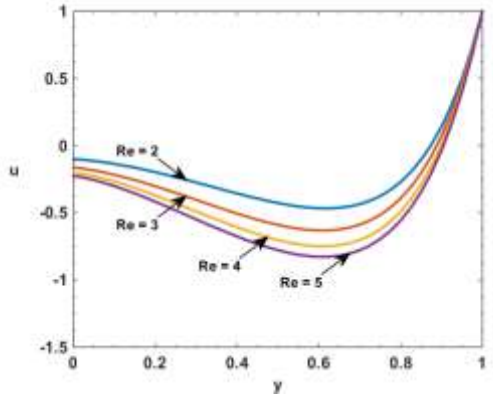

Figure 6: *Main velocity u vs y for λ = 5, Gr = 2.5, Pr = 2, m = 1.5, h = 0.5, Λ = 0.2, f = 0.2, z = 0.0, t = 0.0, ε = 0.05*

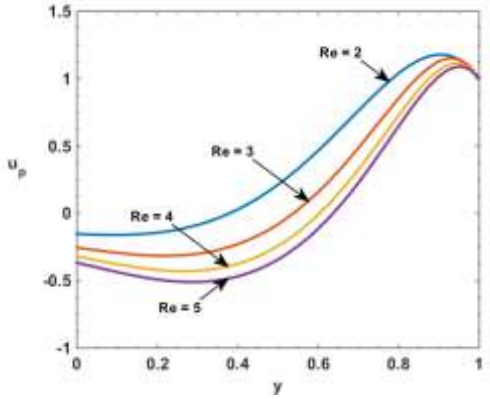

Figure 7: *Main particle velocity u_p vs y for λ = 5, Gr = 2.5, Pr = 2, m = 1.5, h = 0.5, Λ = 0.2, f = 0.2, z = 0, t = 0.0, ε = 0.05*

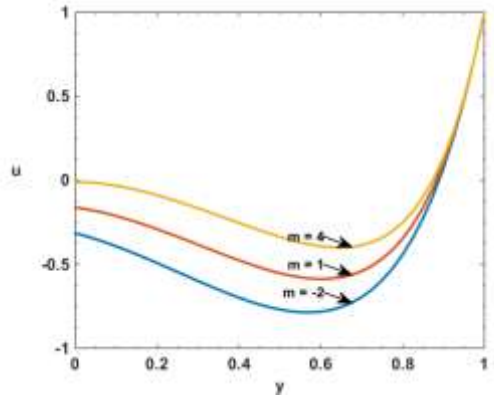

Figure 8: *Main velocity u vs y for λ = 5, Re = 2.5, Pr = 2, Gr = 2.5, h = 0.5, Λ = 0.2, f = 0.2, z = 0.0, t = 0.0, ε = 0.05*

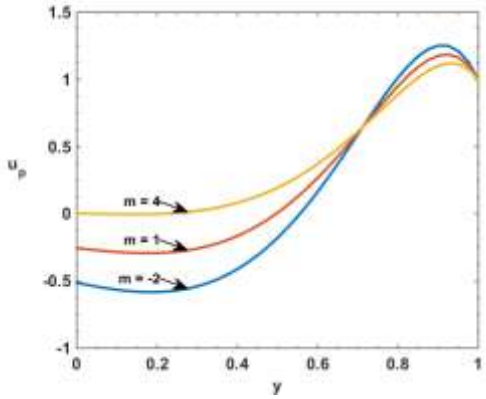

Figure 9: *Main particle velocity u vs y for λ = 5, Re = 2.5, Pr = 2, Gr = 2.5, h = 0.5, Λ = 0.2, f = 0.2, z = 0.0, t = 0.0, ε = 0.05*

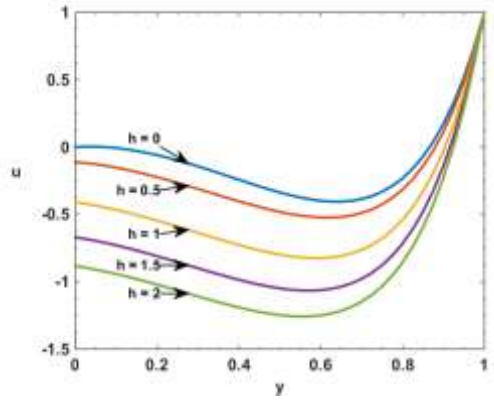

Figure 10: *Main velocity u vs y for λ = 5, Re = 2.5, Pr = 2, Gr = 2.5, m = 2, f = 0.2, Λ = 0.2, z = 0.0, t = 0.0, ε = 0.05*

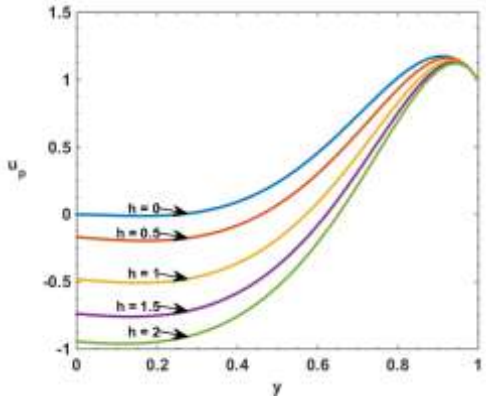

Figure 11: *Main particle velocity u_p vs y for λ = 5, Re = 2.5,Pr = 2, Gr = 2.5, m = 2, f = 0.2, Λ = 0.2, z = 0.0, t = 0.0, ε = 0.05*

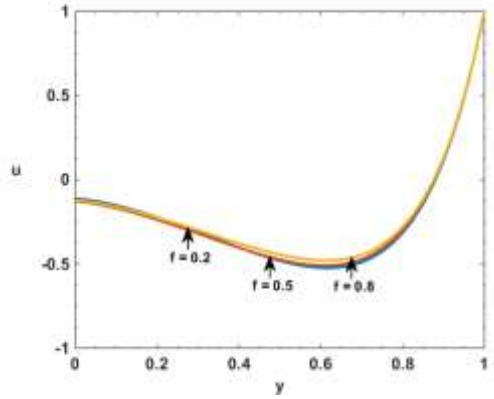

Figure 12: *Main velocity u vs y for λ = 5, Re = 2.5, Pr = 2,Gr = 2.5, m = 2, h = 0.5, Λ = 0.2, z = 0.0, t = 0.0, ε = 0.05*

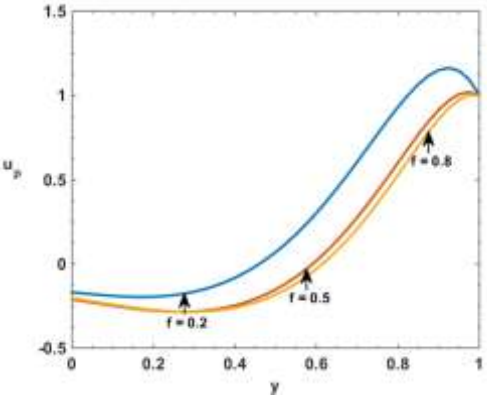

Figure 13: *Main particle velocity u vs y for λ = 5, Re = 2.5,Pr = 2, Gr = 2.5, m = 2, h = 0.5, Λ = 0.2, z = 0.0, t = 0.0, ε = 0.05*

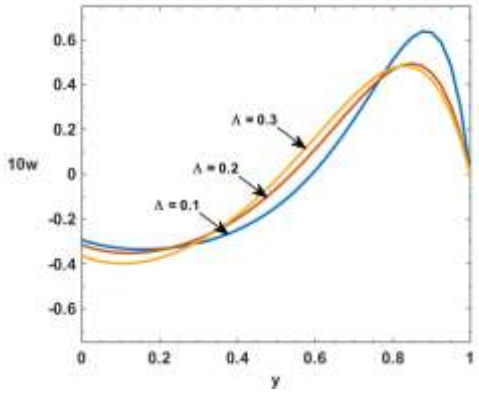

Figure 14: *Cross-flow velocity w vs y for λ = 5, Re = 2.5, Pr = 2, Gr = 10, m = 1.5, h = 0.5, f = 0.2, z = 0.0, t = 0.0, ε = 0.05*

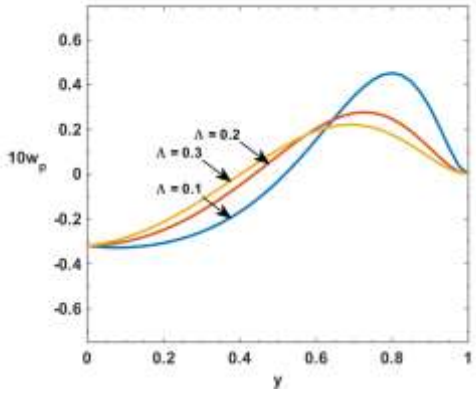

Figure 15: *Cross-flow velocity w_p vs y for λ = 5, Re = 2.5, Pr = 2, Gr = 10, m = 1.5, h = 0.5, f = 0.2, z = 0.0, t = 0.0, ε = 0.05*

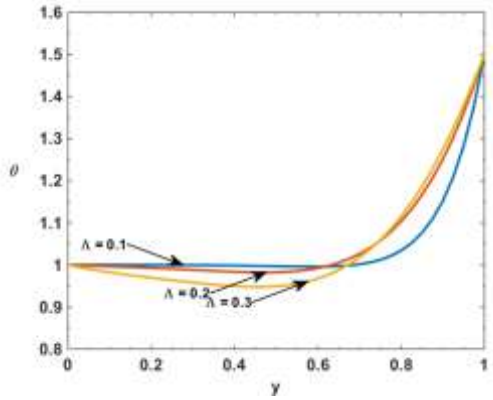

Figure 16: *Temperature θ vs y for λ = 5, Re = 2. 5, Pr = 2, Gr = 10, m = 1.5, h = 0.5, f = 0.2, z = 0.0, t = 0.0, ε = 0.05*

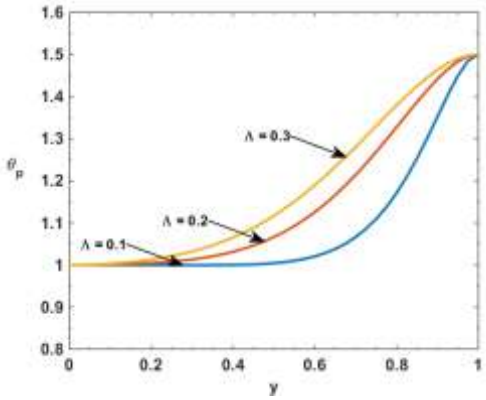

Figure 17: *Particle temperature θ_p vs y for λ = 5, Re = 2.5,Pr = 2, Gr = 10, m = 1.5, h = 0.5, f = 0.2, z = 0.0, t = 0.0, ε = 0.05*

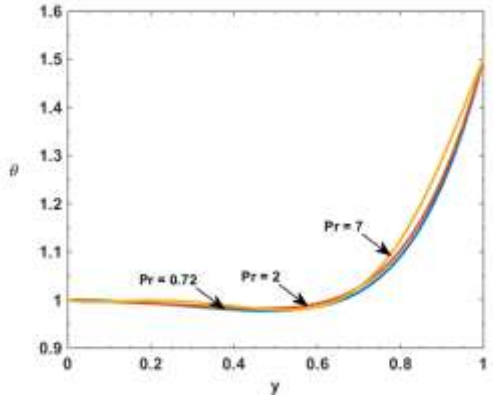

Figure 18: *Temperature θ vs y for λ = 5, Re = 2.5, Gr = 1, m = 1.5, h = 0.5, Λ = 0.2, f = 0.2, z = 0, t = 0.0, ε = 0.05*

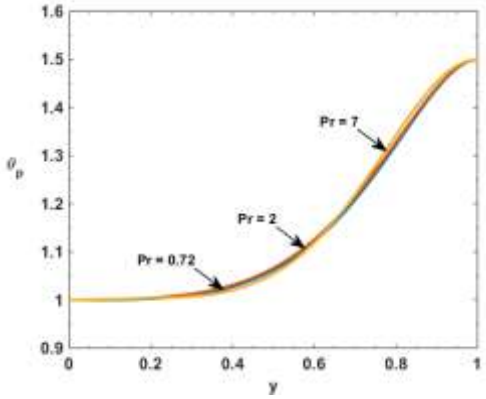

Figure 19: *Particle temperature θ_p vs y for λ = 5, Re = 2.5, Gr = 1, m = 1.5, h = 0.5, Λ = 0.2, f = 0.2, z = 0, t = 0.0, ε = 0.05*

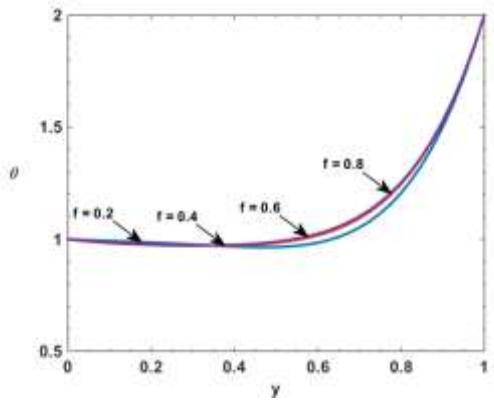

Figure 20: *Temperature θ vs y for $\lambda = 5$, $Re = 2.5$, $Pr = 2$, $Gr = 2.5$, $m = 2$, $h = 0.5$, $\Lambda = 0.2$, $z = 0.0$, $t = 0.0$, $\varepsilon = 0.05$*

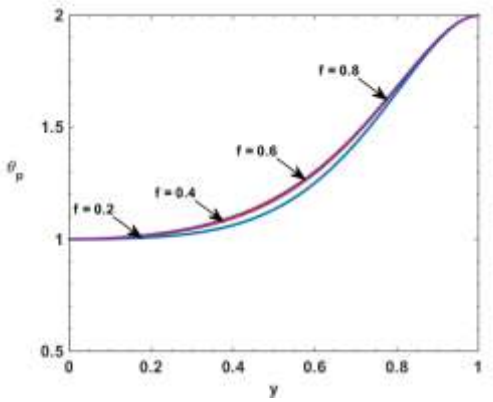

Figure 21: *Particle temperature θ_p vs y for $\lambda = 5$, $Re = 2.5$,$Pr = 2$, $Gr = 2.5$, $m = 2$, $h = 0.5$, $\Lambda = 0.2$, $z = 0.0$, $t = 0.0$, $\varepsilon = 0.05$*

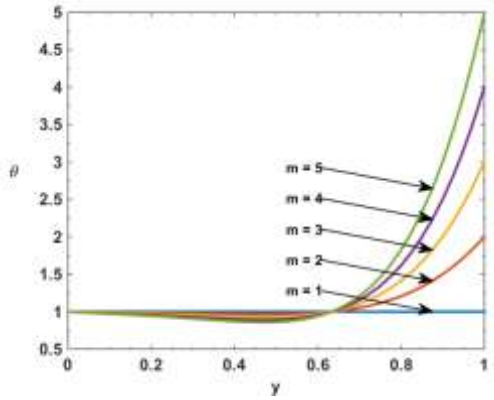

Figure 22: *Temperature θ vs y for $\lambda = 5$, $Re = 2.5$, $Pr = 2$, $Gr = 2.5$, $h = 0.5$, $\Lambda = 0.2$, $f = 0.2$, $z = 0.0$, $t = 0.0$, $\varepsilon = 0.05$*

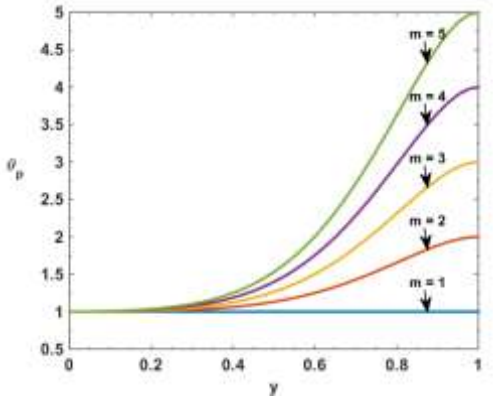

Figure 23: *Particle temperature θ_p vs y for $\lambda = 5$, $Re = 2.5$,$Pr = 2$, $Gr = 2.5$, $h = 0.5$, $\Lambda = 0.2$, $f = 0.2$, $z = 0.0$, $t = 0.0$,$\varepsilon = 0.05$*

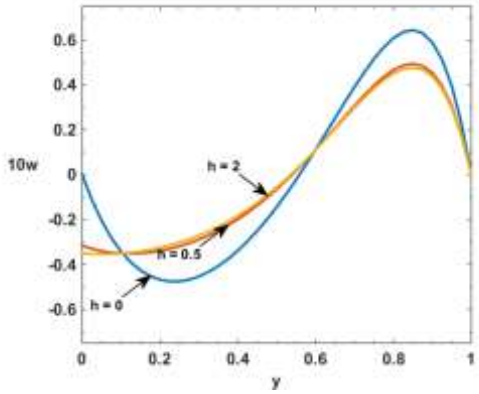

Figure 24: *Cross-flow velocity w vs y for $\lambda = 5$, $Re = 2.5$, $Pr = 2$, $Gr = 2.5$,$m = 2$, $f = 0.2$, $\Lambda = 0.2$, $z = 0.0$, $t = 0.0$, $\varepsilon = 0.05$*

Table 1: Comparison of results of the main flow velocity u with Guria and Jana (2006) for λ = 6, Gr = 0, Pr = 0.72, m = 1, h = 0, z = 0.0, t = 0.2, ε = 0.2

y	Guria and Jana (2006)			Present Work		
	Re = 1.5	Re = 2.0	Re = 2.5	Re = 1.5	Re = 2.0	Re = 2.5
0	0.0000	0.0000	0.0000	0.0000	0.0000	0.0000
0.25	0.3841	0.4359	0.4877	0.3961	0.4462	0.4963
0.5	0.6660	0.7191	0.7670	0.6771	0.7197	0.7616
0.75	0.8640	0.8936	0.9189	0.8933	0.8990	0.9116
1.0	1.0000	1.0000	1.0000	1.0000	1.0000	1.0000

Table 2: Shear stress due to main flow at y = 0 for Gr = 2.5, Pr = 0.72, m = 2, h = 0.5, f = 0.2, Λ = 0.2, z = 0.0, t = 0.0, ε = 0.05

Re	Re_x			$\tan\phi_x$		
	λ = 1	λ = 5	λ = 10	λ = 1	λ = 5	λ = 10
2	3.1778	2.4314	6.8542	-1.6375	-1.0331	-0.7992
3	8.2985	2.3730	2.6252	-3.5349	-0.2738	-0.5452
4	2.3332	2.6268	2.5056	0.1015	0.1042	0.0259
5	1.5035	2.5209	2.7149	0.2807	0.3056	0.2331

Table 3: Shear stress due to main flow at y = 0 for Re = 2.5, Pr = 0.72, λ = 5, h = 0.5, f = 0.2, Λ = 0.2, z = 0.0, t = 0.0, ε = 0.05

Gr	Re_x			$\tan\phi_x$		
	m = 0	m = 1	m = 2	m = 0	m = 1	m = 2
-10	7.7709	1.5828	9.0747	-0.13648	-9.09245	-0.5217
-5	3.8386	0.7944	4.5781	-0.13916	-5.82967	-0.51467
0	0.0959	0.0959	0.0959	0.076986	0.076986	0.076986
5	4.0261	0.7997	4.4160	-0.12881	14.02991	-0.54383
10	7.9585	1.5881	8.9126	-0.13131	87.58858	-0.53627

Table 4: Shear stress due to main flow at y = 0 for Re = 2.5, Pr = 0.72, Gr = 2.5, λ = 5, m = 2, h = 0.5, z = 0.0, t = 0.0, ε = 0.05

F	Re_x			$\tan\phi_x$		
	Λ = 0.1	Λ = 0.2	Λ = 0.3	Λ = 0.1	Λ = 0.2	Λ = 0.3
0.2	1.2050	2.1679	5.1606	0.5183	-0.5595	6.4725
0.4	0.9101	1.1652	2.2303	0.3784	-0.1564	1.6247
0.6	0.7342	0.8979	2.5938	0.2685	0.0176	0.2532

Table 5: Shear stress due to main flow at y = 0 for Re = 2.5, Pr = 0.72, Gr = 2.5, λ = 5, m = 2, f = 0.2, Λ = 0.2, z = 0.0, t = 0.0, ε = 0.05

H	Re_x	$\tan\phi_x$
0	10.4774	0.4314
1	1.2773	-0.6834
2	0.6908	-1.6827

Table 6: Shear stress due to cross flow at y = 0 for Re = 2.5, Pr = 0.72, Gr = 2.5, m = 2, h = 0.5, f = 0.2, z = 0.0, t = 0.0, ε = 0.05

Λ	Re_z			$\tan\phi_z$		
	Λ = 0.1	Λ = 0.2	Λ = 0.3	Λ = 0.1	Λ = 0.2	Λ = 0.3
1	0.2370	0.2980	0.5330	-0.0714	0.5700	1.4634
5	1.1948	1.2739	1.4556	-0.1876	-0.1279	0.0396
10	2.4604	2.5861	2.8129	-0.3766	-0.4922	-0.4343

Table 7: Shear stress due to cross flow at y = 0 for Re = 2.5, Pr = 0.72, Gr = 2.5, λ = 5, m = 2, f = 0.2, Λ = 0.2, z = 0.0, t = 0.0, ε = 0.05

H	Re_z	$\tan \phi_z$
0	10.0484	-0.2211
1	0.6798	-0.1217
2	0.3518	-0.1183

Table 8: Nusselt number at y = 0 for Gr = 2.5, Pr = 0.72, m = 2, h = 0.5, f = 0.2, Λ = 0.2, z = 0.0, t = 0.0, ε = 0.05

Re	Re_T			$\tan \phi_T$		
	λ = 1	λ = 5	λ = 10	λ = 1	λ = 5	λ = 10
2	2.5207	4.3771	5.7800	-0.8105	0.0364	0.3587
3	4.4035	3.9331	4.2636	-0.2052	0.0802	0.2368
4	3.4002	3.7135	3.9340	0.0456	0.1109	0.1834
5	3.5436	3.7250	3.9066	0.0269	0.0949	0.1486

Table 9: Nusselt number at y = 0 for Re = 2.5, Pr = 0.72, Gr = 2.5, λ = 5, f = 0.2, Λ = 0.2, z = 0.0, t = 0.0, ε = 0.05

H	Re_T			$\tan \phi_T$		
	m = 0	m = 2	m = 3	m = 0	m = 2	m = 3
0	6.6486	6.6486	13.2972	0.1812	0.1812	0.1812
1	3.9439	3.9439	7.8878	0.0322	0.0322	0.0322
2	3.8559	3.8559	7.7117	0.0210	0.0210	0.0210

Table 10: Nusselt number at y = 0 for Re = 2.5, Pr = 0.72, Gr = 2.5, λ = 5, m = 2, h = 0.5, z = 0.0, t = 0.0, ε = 0.05

f	Re_T			$\tan \phi_T$		
	Λ = 0.1	Λ = 0.2	Λ = 0.3	Λ = 0.1	Λ = 0.2	Λ = 0.3
0.2	0.1263	4.1053	10.2522	0.1623	0.0509	-0.0210
0.4	0.0574	1.9914	5.8892	0.1695	0.0730	0.0653
0.6	0.0364	1.4098	4.9051	0.1477	0.0901	0.1912

Table 11: Nusselt number at y = 0 for Re = 2.5, Gr = 2.5, λ = 5, m = 2, h = 0.5, f = 0.2, Λ = 0.2, z = 0.0, t = 0.0, ε = 0.05

Pr	Re_T	$\tan \phi_T$
0.72	4.1053	0.0509
2.0	4.5539	0.0681
7.0	7.3351	0.0900

REFERENCES

[1] Ahmed S., Kalita K. and Chamkha A. J., "Analytical and numerical solution of three-dimensional channel flow in presence of a sinusoidal fluid injection and a chemical reaction", *Ain Shams Engineering Journal*, Vol. 6, pp. 691-701, 2015.

[2] Choi C. K., Chung T. J. and Kim M. C., "Buoyancy effects in plane Couette flow heated uniformly from below with constant heat flux", *International Journal of Heat and Mass Transfer*, Vol. 47, pp. 2629–2636, 2004.

[3] Datta N. and Mishra S. K., "Unsteady Couette Flow and Heat Transfer in a Dusty Gas", *Int. Comm. heat and mass transfer*, Vol. 10, pp. 153-162, 1983.

[4] Eckert E. R. G., "Heat and Mass Transfer", *McGraw-Hill*, New York, 1958.

[5] Gireesha B. J., Chamkha A. J., Vishalakshi C. S. and Bagewadi C. S., "Three-dimensional Couette flow of a dusty fluid with heat transfer", *Applied Mathematical Modelling*, Vol. 36, pp. 683-701, 2012.

[6] Govindarajan A., Ramamurthy V. and Sundarammal K., "3D couette flow of dusty fluid with transpiration cooling", *Journal of Zhejiang University SCIENCE A*, Vol. 8, pp. 313-322, 2007.

[7] Guria M. and Jana R. N., "Three-dimensional fluctuating Couette flow through the porous plates with heat transfer", *International Journal of Mathematics and Mathematical Sciences*, pp. 1-18, 2006.

[8] Jiji L. M. and Danesh-Yazdi A. H., "Flow and heat transfer in a micro-cylindrical gas–liquid Couette flow", *International Journal of Heat and Mass Transfer*, Vol.54, pp. 2913–2920, 2011.

[9] Saravanakumar T., Sakthivel R., Selvaraj P, and Marshal Anthoni S., "Dissipative analysis for discrete-time systems via fault-tolerant control against actuator failures", Complexity, Vol. 21, pp. 579-592, 2016.

[10] Singh K. D., "Three-dimensional Couette flow with transpiration cooling", *Journal of Applied Mathematical Physics*, Vol. 50, pp. 661-668, 1999.

[11] Zhang Y., "Effect of wall surface modification in the combined Couette and Poiseuille flows in a nano channel", *International Journal of Heat and Mass Transfer*, Vol. 100, pp. 672–679, 2016.